Design and performance of the ALMA-J prototype antenna

Nobuharu Ukita[a], Masao Saito[a], Hajime Ezawa[a,b], Bungo Ikenoue[a],

Hideharu Ishizaki[a], Hiroyuki Iwashita[a], Nobuyuki Yamaguchi[a,b],

Takahiro Hayakawa[c,a], and the ATF-J team[*]

[a] National Astronomical Observatory of Japan, Mitaka, Tokyo, Japan
[b] Nobeyama Radio Observatory, Minamimaki, Minamisaku, Nagano, Japan
[c] Institute of Astronomy, The University of Tokyo, Mitaka, Tokyo, Japan

ABSTRACT

The National Astronomical Observatory of Japan has constructed a prototype 12-m antenna of the Atacama Compact Array to evaluate its performance at the ALMA Test Facility in the NRAO VLA observatory in New Mexico, the United States. The antenna has a CFRP tube backup structure (BUS) with CFRP boards to support 205 machined Aluminum surface panels. Their accuracies were measured to be 5.9 µm rms on average. A chemical treatment technique of the surface panels has successfully applied to scatter the solar radiation, which resulted in a subreflector temperature increase of about 25 degrees relative to ambient temperature during direct solar observations. Holography measurements and panel adjustments led to a final surface accuracy of 20 µm rms, (weighted by 12dB edge taper), after three rounds of the panel adjustments. Based on a long term temperature monitoring of the BUS and thermal deformation FEM calculation, the BUS thermal deformation was estimated to be less than 3.1 µm rms.

We have employed gear drive mechanism both for a fast position switching capability and for smooth drive at low velocities. Servo errors measured with angle encoders were found to be less than 0.1 arcseconds rms at rotational velocities below 0.1 degrees s^{-1} and to increase to 0.7 arcseconds rms at the maximum speed of the 'on-the-fly' scan as a single dish, 0.5 deg s^{-1} induced by the irregularity of individual gear tooth profiles. Simultaneous measurements of the antenna motion with the angle encoders and seismic accelerometers mounted at the primary reflector mirror edges and at the subreflector showed the same amplitude and phase of oscillation, indicating that they are rigid, suggesting that it is possible to estimate where the antenna is actually pointing from the encoder readout. Continuous tracking measurements of Polaris during day and night have revealed a large pointing drift due to thermal distortion of the yoke structure. We have applied retrospective thermal corrections to tracking data for two hours, with a preliminary thermal deformation model of the yoke, and have found the tracking accuracy improved to be 0.1 – 0.3 arcseconds rms for a 15-munites period. The whole sky absolute pointing error under no wind and during night was measured to be 1.17 arcseconds rms. We need to make both an elaborated modeling of thermal deformation of the structure and systematic searches for significant correlation among pointing errors and metrology sensor outputs to achieve the stable tracking performance requested by ALMA.

Keywords: Radio telescope, submillimeter

1. INTRODUCTION

The Atacama Large Millimeter Array (ALMA)[1] is an astronomical observatory being built at an elevation of 5000 meters in northern Chile where the atmospheric transmission is good for observations at millimeter and submillimeter wavelengths (0.3 to 10 mm) [2,3]. The array consists of 64 12-m transportable antennas served as an interferometer spread over an area of about 10 km extension. Japanese plan is to provide the ALMA with the Atacama Compact Array (ACA) system that consists of twelve 7-m antennas and four 12-m antennas. The 7-m antennas are packed in a very compact configuration (about 35-m area) to take short-baseline data crucial for large-scale astronomical objects. The 12-m antennas are used to make a single-dish image of an area of the sky that is larger than the beam of the array element

antennas. With these low spatial frequency data from the ACA system, the ALMA can make wide-field high-resolution images with high fidelity.

The specifications imposed for the ALMA 12-m antenna operated in open air during daytime and nighttime are demanding and challenging (see section 2 in this report; also Chapter 4 of ALMA Project Book[4]). NRAO and ESO have built two prototype antennas for the 64 12-m antenna array to evaluate their performance at the ALMA Test Facility (ATF) in the NRAO VLA observatory in New Mexico, the United States. The National Astronomical Observatory of Japan (NAOJ) has also constructed a 12-m antenna of the ACA system at the ATF (Figure 1). The construction started in March 2003 and finished in July 2003. We have installed a radio holography system, a refracting telescope of 10 cm, SIS receivers at 3- and 1-mm bands, 227 temperature sensors, and 10 seismic accelerometers. Since then we have been making test to evaluate its performance under various conditions and to establish necessary techniques to achieve the performance requested for the ALMA antennas.

This report describes the technical specifications and unique features of our 12-m antenna design in section 2. Section 3 focuses on two areas of performance evaluations: the surface accuracy and pointing performance.
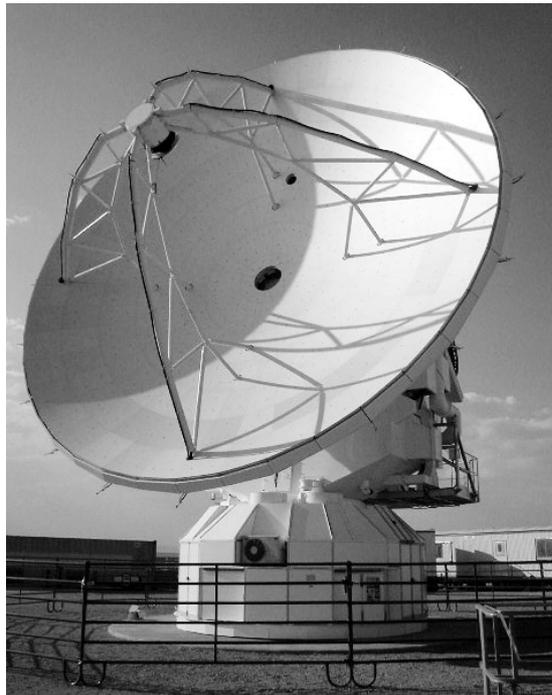

Figure 1. The 12-m ACA antenna of NAOJ at the ATF site

2. DESIGN

2.1 Specification

The technical specifications of our prototype 12-m antenna were identical to those of the two prototype antennas for the 64 element array. We briefly summarize major technical specifications. The antenna employs an alt-azimuth mount. The optical configuration is a Cassegrain arrangement with a main dish f/D ratio of 0.4. Its antenna close packing distance without any possibility of collision is 15 m. The antennas are operated in the observing frequency range from 30 GHz to 950 GHz and therefore the specification requires 25 μm root sum of the squares (rss) as the total antenna surface accuracy. This number includes contribution from both the primary and the secondary reflector. The error budget allocates 10 μm rms for the radio holography measurement. The non-repeatable pointing error for "absolute" pointing on

the whole sky shall not exceed 2.0 arcseconds rss. The non-repeatable "offset" pointing and tracking error shall not exceed 0.6 arcseconds rss over a solid angle of 2 degrees radius and over a 15 minute period. These specifications shall be met under the conditions of an elevation angle range of 2 – 89.8 degrees, ambient temperature range of -20 C to +20 C, wind speed of 9 m s^{-1} (nighttime) and 6 m s^{-1} (daytime), and full solar heating from any direction (primary operating condition).

The antenna has a fast position switching capability to switch 1.5 degrees and settle to within 3 arcseconds in less than 1.5 seconds which enables rapid phase calibration of the array. The drive mechanism can move the antenna at a maximum speed of 6 deg s^{-1} in azimuth and 3 deg s^{-1} in elevation, with a maximum acceleration of 24 deg s^{-2} in azimuth and 12 deg s^{-2} in elevation. The repeatable path length shall not change by more than 20 μm when the antenna moves between any two points 2 degrees apart. The non-repeatable path length must be less than 15 μm rss under the primary operating condition. Direct observations of the sun will be allowed and the primary surface will have a suitable surface treatment to prevent solar heating damage to the subreflector support legs and subreflector.

In the 'on-the-fly' (OTF) total power mapping mode, the antenna scans on the sky at a rate of up to 0.5 deg s^{-1} across a large source. As it scans across the source, it is not necessary for the position at any time to be precisely a pre-commanded position. It is sufficient to simply know where the antenna is actually pointing.

2.2 Design of the ACA 12-m antenna

The basic design concept of our 12-m antenna is similar to that of the 10-m telescope[5] of Atacama Submillimeter Telescope Experiment (ASTE) project. These designs have aimed to have them good performance in severe environments, namely in open air under wind and thermal load. The former one should be taken care of in terms of stiffness or rigidity of the structure. The latter one is handled by use of low thermal expansion materials such CFRP or invar metal. Its backup structure (BUS) consists of an invar central hub, CFRP tubes, invar joints, and CFRP boards. The thermal expansion coefficient of all these components is 2 x 10^{-6}. To keep BUS temperature as uniform as possible, 16 blowers are installed. The surface consists of seven rings of machined aluminum panels whose average accuracy was 5.9 μm rms measured on 3 cm x 3 cm grid points. The total number of panels is 205. On the CFRP board, each panel is supported with three adjusters in order to avoid distortion of the panel in the panel setting. A chemical treatment technique of the surface panels has successfully applied to scatter the solar radiation. A subreflector temperature increase of 25 degrees relative to ambient temperature was observed during direct solar observations. The surface accuracy of a 75-cm subreflector was measured to be 3.3 μm rms.

The antenna has a steel mount structure with 3-point connection to concrete foundation, each foot being fixed with a hydraulic jack. This part houses an antenna control unit, motor drivers, UPS, an azimuth cable wrap, and others. We have employed gear drive mechanism both for a fast position switching capability and for smooth drive at low velocities. For the elevation drive, the antenna has a double sector gear with two angle encoders at the both sides of the yoke arms. The angle encoders are multi-pole resolvers with a 25-bit resolution[6] that have demonstrated their high performance on the ASTE 10-m antenna these four years. Laboratory measurements at the manufacturer of the encoders showed accuracies of 0.023 - 0.044 arcseconds rms. The two resolvers are used not to twist the yoke arms by the double sector gear drive. Our metrology system consists of three subsystems; (1) a reference structure built on an azimuth bearing in the yoke to measure the deflection and thermal expansion of the yoke arms, (2) tiltmeters to measure the tilt of the reference structure base-plate, and (3) temperature sensors in the primary reflector, subreflector quadripod, and yoke. The first one is to cope with a tilt and twist of the yoke arms due to wind and thermal loadings on them. The second one is necessary to measure a small change of the azimuth rotation axis tilt that is caused by changes of mechanical and environmental loadings on the mount structure. Temperature monitoring data from the third subsystem are used to make pointing corrections using a semi-empirical pointing coefficient matrix.

3. PERFORMANCE EVALUATION

To evaluate the performance of the antenna, we have installed a radio holography system, an optical pointing telescope (OPT) of 10 cm, SIS receivers at 3- and 1-mm bands, and seismic accelerometers. We have also used monitor data of the metrology system such as linear encoders on the reference structure, tiltmeters, and temperature sensors.

3.1 Surface Accuracy

3.1.1 Holography Measurement

The ASTE holography system is adopted which sets the main receiver at the Cassegrain focus and locates the reference receiver on the rear side of the subreflector. The advantages of the Cassegrain layout are that it is relatively easy to measure the amplitude and phase pattern of a main corrugated horn with having a narrow beamwidth. The phase pattern of the main horn affects on the final holography surface map. Further, our holography measurement in principle includes both the primary and secondary reflector. On the other hand, unwanted radial ripple patterns appeared on the surface error map is considered to be disadvantage in the Cassegrain system. The prime focal holography system does not suffer from these ripple patterns while it requires a horn antenna covering a wide range of angle. It is not easy to measure the radiation pattern of such a horn accurately.

The transmitter is mounted on a tower at the VLA site and is at a distance of 377m operating at 95.3 GHz. The observing elevation is 7.45 degree. All the measurements are mapped on-the-fly typically mapping a 64 x 64 raster taking about 20 minutes. The final IF frequency is about 1 kHz after frequency conversion twice. Individual signal from the reference and main receiver are sampled at the 24 bit A/D board mounted in the receiver cabin and cross spectrums are recorded in a binary file. Then, the data are Fourier inverted and corrected for the near-field phase profile to produce the aperture phase distribution. After fitting DC and gradient errors, the phase residuals are converted to surface deviations which are used to adjust the panels. The data acquisition and analysis use an enhanced version of a software package originally developed by the ASTE team.

The panel adjusters are designed such that the thermal effect on the adjusters causing the minimum deformation of the panel. The panel setting was done with a dedicated tool from the front side. This automatic panel setting tool identifies individual panel adjuster by reading a barcode attached adjacent to each adjuster. Upon identification of the panel adjuster it performs the adjuster setting in automatic mode to a value previously stored in the tool. The surface was improved from 122 μm rms to 20 μm rms after three rounds of the panel adjustments. It typically took 6 hours to complete the entire dish adjustment with two personnel and a manlift.
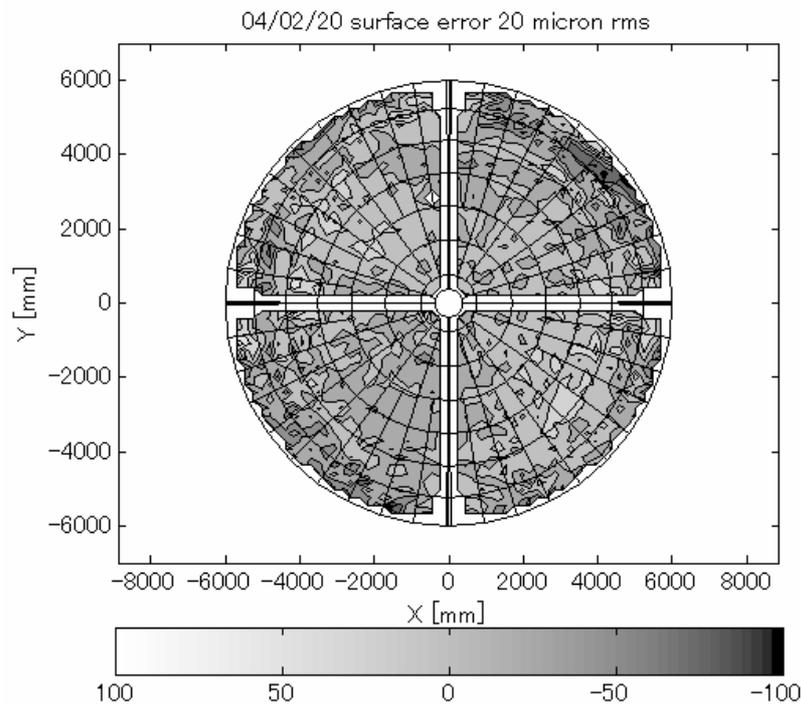

Figure 2. A surface error obtained from a holography measurement

Figure 2 shows the surface error map of the 12-m main reflector. The final surface accuracy weighted by 12dB edge taper was 20 μm rms after removing radial ripple patterns mainly caused by the subreflector diffraction. The short-term repeatability of the measurements is as good as 11 μm rms in the entire dish, 5.5 μm rms in the area of r < 5.2 m. Fitting to the final surface map suggests further panel setting of 15 μm rms and if set perfectly the resultant surface error is estimated to be 13 μm rms.

3.1.2 Thermal deformation of the primary reflector

FEM analysis of thermal deformation of the primary reflector was performed. The calculation is based on the temperature measurements on the back-up structure over 170 days. The ambient temperature over the measuring period ranged from -5 to 30 degrees. The amplitude of the temperature variation is roughly same as the ALMA primary condition (-20 < T < 20 degrees) with an offset of 15 degree and thus we consider the results applicable to the ALMA primary condition. Among more than the 227 temperature sensors, 55 sensors are located on the BUS, 25 ones mounted on the central hub, and 32 ones are mounted on the CFRP board.
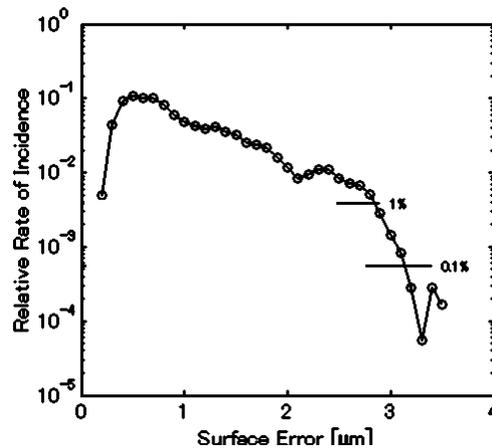

Figure 3. Histogram of thermal deformation of the primary reflector

Figure 3 shows a histogram of the results of thermal deformation analysis. The figure demonstrates that in most cases the surface deformation is less than 2 μm rms and that the surface error is less than 3.1 μm rms in 99.9 % of the measurement period. The number obtained in the present estimate meets the error budget in the design study.

3.2 Pointing Accuracy

Pointing measurements shown below have been made with only the tiltmeters among our metrology system being in full operation. The reference structure and thermal correction subsystems (section 2.2) are under study to find out a proper correction matrix, although they had been individually tested both in Japan and at the ATF.

3.2.1 Tracking accuracy – servo error –

The angle encoder of each axis is one of the fundamental devices to characterize the antenna motion. We have measured servo errors (encoder readout – commanded angle) at several different rotational velocities (Figure 4-a). In a low rotational velocity range the servo error was measured about 0.02 arcseconds smaller than the encoder errors. We found the servo error significantly depends on the rotational velocity (Figure 4-a). At sidereal rate or interferometric mosaicking rate of 0.05 deg s^{-1}, the tracking error was obtained to be about 0.1 arcseconds rms. At the maximum speed of OTF scan as a single dish, 0.5 deg s^{-1}, its error increases to 0.7 arcseconds rms. The error pattern was of a sine wave with a frequency of 0.25 Hz and an amplitude of about 0.8 arcseconds (Figure 4-b; solid line). The observed frequency corresponds to the gear mesh frequency at this rotational velocity, suggesting that the source of error is the irregularity of individual gear tooth profiles. The spectra observed with seismic accelerometers mounted at the primary reflector mirror edges and at the subreflector showed the same amplitude (Figure 4-b; broken line) and phase, indicating that the primary reflector, subreflector, and elevation axis are rigid and behave as a single structure. Therefore it is possible to estimate where the antenna is actually pointing from the encoder readout.
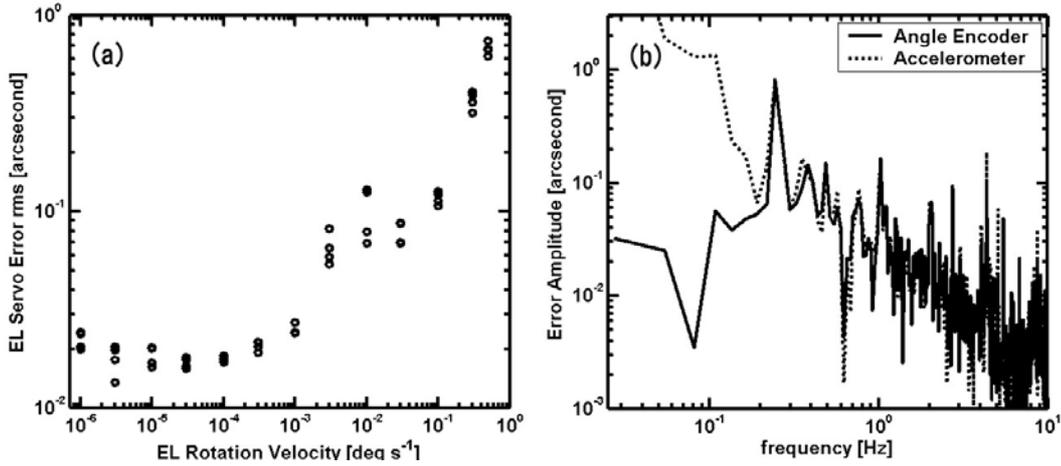
Figure 4. (a) Servo errors versus rotation velocity, (b) spectra of pointing errors observed with the angle encoders (solid line) and seismic accelerometers in the primary mirror (broken line) at a rotational velocity of 0.5 degree s^{-1}. The data points of the accelerometers below 0.15 Hz correspond to a noise floor (v^{-2}) of the accelerometer measurement system.

3.2.2 Tracking accuracy – thermal drift -

We have performed tracking tests with the OPT mounted on the BUS. We have made the telescope according to a design by NRAO. It has an objective lens of 10 cm with a focal length of 920 mm and a 2X extender lens that gives a final focal length of 1840 mm on a peltier cooled CCD camera. The telescope tube and support structure are made of invar to minimize flexure due to thermal deformation. A red filter (R64) was used to make observations during daytime. An effective wavelength was estimated to be 740 nm from response curves of the CCD and the filter. We have made measurements towards stars brighter than $m_v < 3.5$ magnitude. The video signal at 30 frames per second was digitized with a frame grabber of 8 bit, and recorded on a PC in a bitmap image format of 640 x 480 pixels. Final plate scales and an image rotation angle were measured by observing Polaris on 0.03 x 0.03 degree grid points in azimuth and elevation. The plate scales were found to be 1.16 arcsecond per image pixel in both horizontal and vertical.

Measurement accuracies were estimated by analyzing stellar image motion recorded for 50 – 100 frames at 30 Hz towards stars for whole sky pointing measurements (see section 3.2.4) and those for 300-second star tracking measurements. Standard deviations of image motion were found to increase with square root of air mass in most of the measurements. FFT spectra of stellar image motion for the longer measurement period showed a Kolmogorov -2/3 turbulence relationship. These suggest that the measurement accuracies are limited by the atmospheric optical seeing at the ATF site. Typical image motions at zenith estimated for data in March 2004 were 0.4 – 0.6 arcseconds rms for the 50 frames, which indicates Fried's lengths of 16 – 10 cm, comparable to those measured at nearby observatories[7, 8].

Continuous tracking accuracies were tested by observing several stars in different azimuth and elevation for one hour or two. Upper panels of Figure 5 show the measured pointing errors derived from an average of 300 frames taken in 60 seconds towards β Leo for two hours during night. The standard deviations of 300 frames were found to decrease with elevation angle, and the mean value of standard deviations was about 0.6 arcsecond. We estimated measurement accuracies of individual points in Figure 5 to be 0.2 arcseconds assuming the Kolmogorov relationship. The pointing drifts in the two upper panels have been suspected of thermal deformation of the antenna structure. Three rounds of continuous tracking on Polaris during day and night were carried out in March and June 2004. Preliminary analyses have suggested a good correlation between pointing errors in elevation and temperature differences among front- and back-side of the yoke arms, and also possible correlations between pointing errors in azimuth and temperatures of the tiltmeter on the azimuth axis that is used for the real-time tilt correction. Using these correlations, we have applied retrospective thermal corrections to the data (lower two panels of Figure 5). Assuming pointing corrections made every 15 minute, pointing errors (rms) of the lower panels were improved to be 0.1 – 0.3 arcseconds, except for the first 15 minute period in elevation (0.8 arcsecond rms). These results clearly suggest that we need further improvements, because thermal correction error is assigned to be 0.0 (nighttime) - 0.4 (daytime) arcsecond specified in our pointing error budget. We

shall make further measurements and thermal correction tests with a real-time thermal pointing correction module that has already been implemented in the antenna control unit.
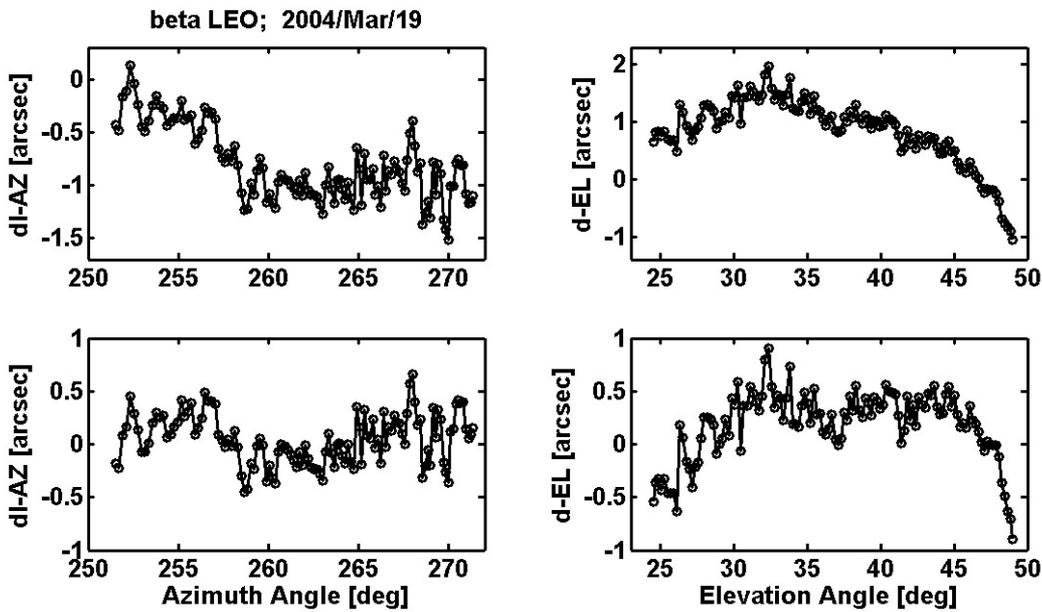

Figure 5. Pointing drift due to thermal load on the yoke structure. Upper panels display observed pointing errors in azimuth (left) and elevation (right). Lower panels show pointing errors after retrospective thermal pointing corrections.

3.2.3 Offset pointing error

We have observed two stars with OPT to simulate a pointing stability test of fast position switching observations in which a target- and reference-source are 2 degrees apart on the sky (maximum). Since there is only a few pairs of bright stars that meet the condition, we have selected ξ Dra and γ Dra that are about 9 degrees apart. We have observed the two stars alternately every 40 seconds (Figure 6). The measured errors were 0.3 arcseconds (rms) in azimuth, 0.5 arcseconds (rms) in elevation. The radial error is 0.6 arcseconds, including the error of the individual measurements of 0.42 arcseconds rms.
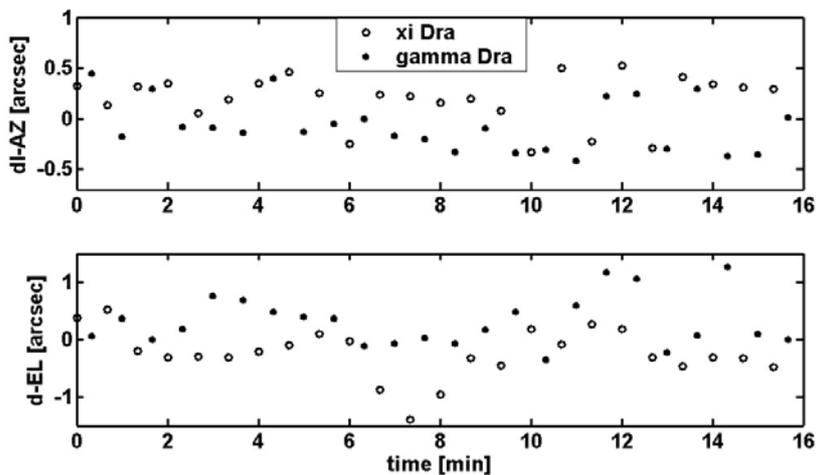

Figure 6. Offset pointing error

3.2.4 Whole sky pointing accuracy

The ALMA "absolute" pointing accuracy for the whole sky is 2.0 arcseconds rss. The first step is to establish a good pointing model that describes repeatable pointing error characteristics with a simple formula. Mangum[9] has discussed additional pointing equation terms to the terms of a basic telescope pointing model that characterizes axis-alignment errors and the elastic flexure of an azimuth-elevation mount telescope. We introduced terms specific to our antenna. They are terms to compensate scale errors of the tiltmeters on the azimuth axis[9] and terms in sin(nAz) and cos(nAz), n = 2 and 3, for the errors induced by offset loading of the structure above the azimuth bearing on the three-foot mount structure.

Figure 7 shows observed pointing errors for 216 stars observed in 80 minutes (three runs, each of 25 minutes) during night. The pointing model used in the measurements was constructed from the data of 70 stars observed in the previous night. A typical error of each measurement averaged for the 50 frames was estimated to be 0.3 arcseconds in both azimuth and elevation according the Kolmogorov relationship. The pointing errors both in azimuth and elevation in Figure 7 were 0.85 and 0.80 arcseconds rms, respectively. The radial pointing error was 1.17 arcseconds. The residuals after fitting for a new pointing model are 0.72 and 0.75 arcseconds rms. The radial pointing error is slightly improved to 1.05 arcseconds. This radial pointing error of 1.05 arcseconds includes the encoder errors of 0.05 arcseconds (section 2.2), the servo error of 0.14 arcseconds (section 3.2.1), and the errors due to seeing of 0.42 arcseconds, which suggests that a typical error due to non-repeatable and/or local irregularity is about 1.0 arcsecond rms under no wind and night conditions.
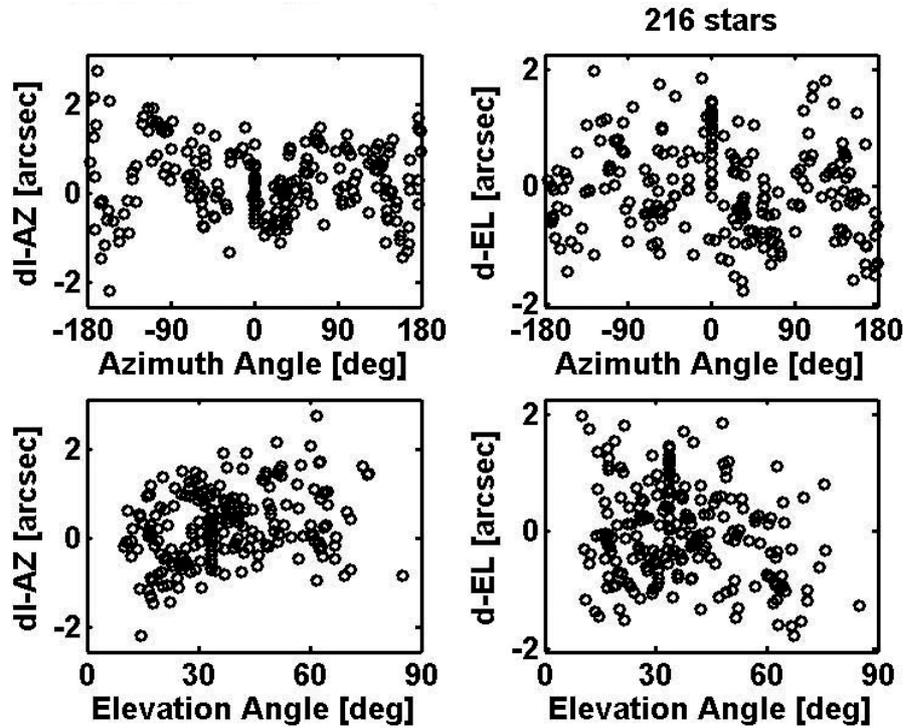

Figure 7. Observed pointing errors in the all sky pointing check

In addition to this non-repeatable component of 1.0 arcsecond, the non-repeatable pointing error for "absolute" pointing includes (1) an error of a pointing model itself, (2) pointing model stability over one month, (3) errors due to wind loadings on the primary reflector (steady component of 0.5 arcseconds and gust component of 0.2 arcseconds from FEM calculations) that our metrology system cannot make any pointing corrections, (4) an residual error of thermal pointing correction (0.4 arcseconds) if our metrology system works well.

In the future work, we have to evaluate the pointing error under windy condition, daytime, and over a long period. We need to make both an elaborated modeling of thermal deformation of the structure such as done on the IRAM 30-m

telescope[11] and systematic searches for significant correlation among pointing errors and metrology sensor outputs to achieve the stable tracking performance requested by ALMA.

ACKNOWLEDGMENTS

REFERENCES

1. M. Tarenghi, "ALMA," in *Ground-based Telescopes, Proc. SPIE* **5489**, in this volume, 2004.
2. S. Matsushita, H. Matsuo, J.R. Pardo, and S.J.E. Radford, "FTS Measurements of Submillimeter-Wave Atmospheric Opacity at Pampa la Bola II : Supra-Terahertz Windows and Model Fitting," *PASJ.* **51**, pp. 603-610, 1999.
3. S. Paine, R. Blundell, D.C. Papa, J.W. Barrett, and S.J.E. Radford, "A Fourier Transform Spectrometer for Measurement of Atmospheric Transmission at Submillimeter Wavelengths," *PASP.* **112**, pp. 108-118, 2000.
4. J. Kingsley, and J. Baars, "ALMA Construction PROJECT BOOK , Chapter 4 Antennas," http://www.alma.nrao.edu/ projectbk/construction/, 2002
5. N. Ukita, R. Kawabe, M. Ishiguro, H. Ezawa, Y. Sekimoto, S. Yamamoto, T. Hasegawa, K. Miyawaki, S. Matsumoto, "NRO 10m submillimeter telescope," in *Radio Telescopes, Proc. SPIE* **4015**, pp 177-184, 2000.
6. N. Ukita, H. Ezawa, H. Mimura, A. Suganuma, K. Kitazawa, T. Masuda, N. Kawaguchi, R. Sugiyama, K. Miyawaki, "A High-Precision Angle Encoder for a 10-m Submillimeter Antenna," in *Publ. of the Natl Astron. Obs. Japan* **6**, pp. 59-64, 2001
7. B.L. Ulich, and W. Davison, "Seeing Measurements on Mount Graham," *PASP.* **97**, pp. 609-615, 1985.
8. D.J. Neimeier, "Optical Strength of Atmospheric Turbulence," Master Thesis of New Mexico Institute of Mining and Technology, April 2003.
9. J.G., Mangum, "A Telescope Pointing Algorithm for ALMA," ALMA Memo #366, http://www.alma.nrao.edu/ memos/index.html, 2001
10. N. Ukita, "Thermal Effects on the Pointing of the Nobeyama 45-m Telescope," in *Publ. of the Natl Astron. Obs. Japan* **5**, pp. 139-147, 1999.
11. A. Greve, M. Bremer, J. Peñalver, P. Raffin, D. Morris, "Improvement of the IRAM 30-m Telescope from Temperature Measurements and Finite Element Calculations," IRAM preprint 574, 2004.